Am J Cancer Res 2022;12(7):3303-3317
www.ajcr.us /ISSN:2156-6976/ajcr0142212

Original Article

CDC20 is a novel biomarker for improved clinical predictions in epithelial ovarian cancer

Xiaoxue Xi[1], Tianyue Cao[1], Yonghong Qian[1], Huiling Wang[1], Songwen Ju[2], Youguo Chen[3], Ting Chen[1], Jian Yang[1], Biaoquan Liang[1], Shunyu Hou[1]

[1]Department of Obstetrics and Gynaecology, The Affiliated Suzhou Hospital of Nanjing Medical University, Suzhou Municipal Hospital, Gusu School, Nanjing Medical University, Suzhou 215002, Jiangsu, China; [2]Central Laboratory, Nanjing Medica University Affiliated Suzhou Hospital, Suzhou 215128, Jiangsu, China; [3]Department of Obstetrics and Gynaecology, The First Affiliated Hospital of Soochow University, Suzhou 215006, Jiangsu, China

Received February 7, 2022; Accepted June 13, 2022; Epub July 15, 2022; Published July 30, 2022

Abstract: Epithelial ovarian cancer (EOC), a common tumor of the female reproductive system, ranks first in fatalities among gynecological malignancies. Most patients find tumors at late stage and have extremely poor prognoses, which necessitates improvements in early detection. This study applied bioinformatic methods to identify potential biomarkers of EOC. First, Gene Ontology (GO) and Kyoto Encyclopedia of Genes and Genomes (KEGG) analyses were performed on differentially expressed genes (DEGs) and hub genes, and a protein-protein interaction (PPI) network was constructed. The network of hub genes was analyzed using GeneMANIA, and an analysis of biological processes was constructed with BINGO. Lastly, hub genes were analyzed for EOC-related oncology using the Oncomine and TCGA databases, and the cBioPortal online platform. Overall, cell division cycle 20 (CDC20) was identified as a key gene in EOC. Short hairpin RNA (shRNA) was used to silence CDC20 to explore its effects on EOC cell proliferation, apoptosis and SRY-related HMG-box 2 (SOX2) expression. DEGs were enriched in pathways related to cell cycle signaling, cancer, progesterone-mediated oocyte maturation, Wnt signaling and P53 signaling. Analysis revealed high expression of CDC20 in EOC tissues and a correlation with histology and tumor grade. CDC20 levels are highest in serous adenocarcinoma, when compared to ovarian clear cell carcinoma, ovarian endometrioid carcinoma and mucinous adenocarcinoma. High CDC20 expression within the tumor is associated with poor EOC prognosis. After silencing *CDC20*, EOC cell proliferation and migration decreased, apoptosis increased, and *SOX2* expression decreased. In conclusion, CDC20 is likely a key biomarker of EOC and may act as an upstream regulator of SOX2 to mediate the SOX2 signaling in the progression of EOC. Future application of CDC20 analysis to early detection may improve prognosis, and it has the potential to be a therapeutic target.

Keywords: Epithelial ovarian cancer, biomarkers, bioinformatics, CDC20, SOX2

Introduction

Epithelial ovarian cancer (EOC) has the highest fatality rate of gynecological malignancies [1]. Due to a lack of typical symptoms in the early stages of EOC, tumors are often at an advanced stage at diagnosis. As such, the lesions show extensive invasion and metastasis, resulting in delayed treatment and poor prognosis [2, 3]. The pathogenesis of EOC is complex and regulated by a variety of oncogenes and tumor suppressor genes [4]. Although multiple ovarian cancer (OC) genes have been identified, the mechanisms of EOC progression remain unclear [5, 6]. Therefore, exploring the key genes and signaling pathways surrounding proliferation and apoptosis of OC cells can provide molecular targets for use in clinical diagnosis and treatment.

Rapid developments in bioinformatics have facilitated the mining of tumor pathogenesis and signaling pathways from a genomic perspective [7, 8]. Here, this study applied bioinformtatic methods to three publicly available microarray datasets (GSE36668, GSE18520 and GSE54388) to find key biomarkers for EOC and, to uncover differentially expressed genes (DEGs) and hub genes in EOC tissue. This study applied further analyses of the DEGs using Gene Ontology (GO) and Kyoto Encyclopedia of Genes and Genomes (KEGG) approaches and

built a protein-protein interaction (PPI) network of DEGs to identify cellular processes impacted in EOC tissue.

Six newly identified hub genes underwent analysis using multiple OC-related oncology resources, including the Oncomine and TCGA databases, and the cBioPortal online platform. Additionally, the network of hub genes and their coexpressed genes were explored using GeneMANIA. Ultimately, one of the hub genes, CDC20, was chosen for further testing as it most closely related to EOC due to its highly expression in EOC tissue and its relation to tumor pathological type, grade and prognosis [9, 10]. Binding of CDC20 activates the anaphase-promoting complex (APC) and forms an E3 ubiquitin ligase complex. APC/C^{CDC20}, which participates in the degradation of downstream substrates, regulates the mitotic cycle and promotes apoptosis [9, 11].

Recent studies report CDC20 involvement in tumor development as a tumor-promoting factor [12-14]. In glioblastomas, CDC20 acts through SOX2 to alter the proliferation, migration, invasion and tumorigenic potential of tumor cells, while blocking the G0/G1 phase of the cell cycle [15, 16]. Thus, CDC20 may participate in EOC progression as an upstream regulator of SOX2. Here, we applied bioinformatic analysis to EOC cell datasets and assayed the impact of CDC20 knockdown on cellular proliferation, apoptosis, and migration, as well as on regulation of SOX2 expression at the gene and protein levels.

Materials and methods

Data downloading and processing

Datasets related to EOC were searched from the public database Gene Expression Omnibus (GEO) (http://www.ncbi.nlm.nih.gov/geo/) using the selection criteria: 1) It was a study sample of EOC tissue; 2) It contained gene expression profiles of mRNA; and 3) It contained complete analysis information. Chip data expression profiles GSE36668, GSE18520, GSE54388 were selected. All are the GPL570 platform (Affymetrix Human Genome U133 Plus 2.0 Array). The GSE36668 dataset contains 4 serous OC samples and 4 normal ovarian samples. The GSE18520 dataset contains 53 serous OC samples and 10 normal ovarian samples. The GSE54388 dataset contains 16 serous OC samples and 6 normal ovarian samples.

Screening for differentially expressed genes (DEGs)

DEGs were screened using the GEO2R software, an interactive web tool that allows users to compare two or more datasets within a GEO series (http://www.ncbi.nlm.nih.gov/geo/geo2r). Probe sets without corresponding gene symbols or genes with more than one probe set were removed or averaged, respectively. $P<0.01$ and the absolute value of logFC (fold change) greater than 2 were considered statistically significant.

GO and KEGG analysis

DAVID, an online bioinformatics database that integrates biological data and analysis tools, provided gene and protein functional information used to annotate the screened OC DEGs (http://david.ncifcrf.gov). The DEGs were both functionally classified according the GO classification project, including molecular functions, cellular processes, and cellular components, and also viewed using KEGG signaling pathway analysis.

Protein-protein interaction (PPI) networks and screening for important modules

PPI networks were predicted using STRING, which displays interacting genes (http://string-db.org). The bioinformatic program, Cytoscape, displays molecular interaction networks while MCODE, a plug-in within Cytoscape, clusters networks based on topology to identify densely connected regions. PPI networks were plotted using Cytoscape, and MCODE was used to determine the most important modules within the PPI network. The selection criteria used are as follows: MCODE scores >5, degree cutoff =2, node score cutoff =0.2, k-Core =2, Max. Depth =100.

Screening and analysis of hub genes

Hub genes were identified using a Cytoscape plug-in, MCODE. The functional relationship network map of hub genes and their co-expressed genes was drawn using GeneMANIA (https://genemania.org). Biological process analysis of hub genes was performed using a

Cytoscape plugin-in, BiNGO. The survival analysis of hub genes was performed on the cBioPortal website (http://www.cbiportal). The online database Oncomine (http://www.oncomine.com) was used to analyze the relationship between gene expression and tumor type and grade.

Cell culture and transfection

The human OVCAR3 OC cell line was obtained from Shanghai Cell Bank (Chinese Academy of Sciences). OC cells were placed in RPMI-1640 medium (Invitrogen, USA) containing 10% FBS and cultured in a 37°C, 5% CO_2 cell incubator. Adherent cells were plated at 1×10^5/well in 6-well plates. The number of cells at the time of transfection was about 2×10^5/well. Cells were transfected using Lipofectamine 2000 (Gema, Shanghai, China) according to the manufacturer's protocol. The experiment was divided into blank control group (control), blank vector group (shRNA NC) and three interference groups (CDC20 shRNA01, CDC20 shRNA02, CDC20 shRNA03) (BioGeek™ Lentiviral Packaging Kit, Hesheng, Beijing, China).

Quantitative real-time polymerase chain reaction (qRT-PCR)

Total RNA was extracted with Trizol (Invitrogen, USA) from the five groups of OC cells. Using 1 μg RNA as template, cDNA was synthesized by qPCR reverse transcription kit. Using 1 μL cDNA as template, the expression levels of *CDC20* and *SOX2* mRNA were detected by qPCR. PCR amplification setting conditions are as follows: Amplification curve: 95°C 5 min 1 cycle; 95°C 5 s, 60°C 31 s 40 cycles; Melting curve: 95°C 15 s, 60°C 30 s, 95°C 15 s. The primer sequences used for PCR amplification are as follows: for CDC20: 5'-GACCACTCCTAGCAAACCTGG-3' (forward), 5'-GGGCGTCTGGCTGTTTTCA-3' (reverse; for SOX2: 5'-TACAGCATGTCCTACTCGCAG-3' (forward), 5'-GAGGAAGAGGTAACCACAGGG-3' (reverse).

Western blot analysis

After addition of lysis buffer to each group of OC cells, total protein was extracted and the protein concentration was measured. 20 μL of the protein sample was loaded and transferred to the membrane after sodium dodecyl sulfate polyacrylamide gel electrophoresis (SDS-PAGE). The samples were blocked at room temperature for 2 hours and incubated overnight with CDC20 and SOX2 monoclonal antibodies (Affinity, USA). After 1 hour incubation with secondary antibody, ECL chemiluminescence was used to determine the expression levels of CDC20 and SOX2 proteins. β-actin was used as an internal reference, and the protein expression level was calculated using the gray value of the target protein divided by the gray value of the β-actin protein.

Cell Counting Kit-8 (CCK8)

After transfection, the five groups of OC cells were plated and the cell density was adjusted to 1000 cells/100 μL. Cell proliferation was assessed after incubation (37°C, 5% CO_2) for various times (24 h, 48 h, 72 h, 96 h, 120 h, 168 h) using the following protocol: 10 μL of CCK8 (Gema, Shanghai, Company) was added to each well, the cells were incubated at 37°C for 4 hours, and the OD was read at 450 nm using a microplate reader.

Annexin-V FITC/PI double staining

Cells were washed twice with PBS (centrifugation at 1000 rpm, 5 min) and 5×10^5 cells were resuspended in 500 μL of Binding Buffer. Next, 5 μL of Annexin V-FITC (KGI, Jiangsu, China) was added followed by 5 μL of Propidium Iodide. After 5-15 min, cell apoptosis was detected by flow cytometry.

Transwell chamber migration assays

Transwell assays were carried out using migration chambers with 8 μm membranes (Millipore, Billerica, MA, USA). The well-grown cells were routinely digested and centrifuged with DMEM medium containing 5% FBS, resuspended and counted, and inoculated into transwell chambers. About 2000 cells were added to each chamber. After 24 h, the cells were gently washed three times with PBS buffer and fixed with 4% paraformaldehyde for 30 min. Cells were stained with hematoxylin, sliced, photographed, and counted.

Statistical analysis

SPSS software (version 23.0) was used for data analysis. Each experiment was repeated at least three times. Measurement data are

expressed as mean ± standard deviation. Western blot results were analyzed and compared by semi-quantitative western blot analysis. The independent samples *t* test was used to compare the differences between two groups, the one-way analysis of variance (*F* test) was used to compare the differences between three groups or more, and the *q* test was used to compare the differences between groups. A difference of $P<0.05$ was considered statistically significant.

Results

DEGs screening

To highlight key genes and pathways involved in EOC, publicly available microarray datasets of EOC tissue underwent bioinformatic analysis. After normalization of the microarray results, DEGs were identified within the datasets using GEO2R software. The program identified 1729 DEGs in GSE54388, 3769 DEGs in GSE36668, and 1151 DEGs in GSE18520 when OC tissue was compared to the normal ovarian tissue within each dataset. Of note, 285 genes were differentially expressed across all datasets (**Figure 1A**), of these DEGs, 130 genes were upregulated between OC tissues and normal ovarian tissue, and 155 genes were downregulated.

GO enrichment and KEGG pathway analysis of DEGs

To uncover the biological functions of DEGs in the EOC microarray datasets, functional and pathway enrichment analysis was performed using DAVID Bioinformatic Resource. GO analysis describes genes across three biological domains: biological processes (BP), cellular component (CC), and molecular function (MF). The BP enriched the DEGs were cell division, mitotic and nuclear division, cell proliferation, positive regulation of RNA polymerase II promoter transcription, and protein localization to the kinetochore (**Table 1**). The CC enriched in the DEGs included the midbody, the spindle, cell surface, spindle microtubule, and the anchoring component of the cell membrane. The MF GO analysis results focused mainly on the binding of sequence-specific DNA, microtubules, kinesin, protein kinase, and heat shock protein (HSP70). Additionally, KEGG pathway analysis showed that DEGs were enriched in the following pathways: cell cycle, cancer, progesterone-mediated oocyte maturation, Wnt signaling, and P53 signaling (**Table 1**).

PPI network and module analysis

The analysis of functional interactions between proteins can provide mechanistic insight into disease occurrence and development. The bioinformatic tool Cytoscape was used to construct a PPI network of the DEGs with important modules within the network highlighted (**Figure 1B**). The most important module identified in the network had 43 nodes and 854 edges (**Figure 1C**). Interestingly, functional analysis of the genes in this module revealed a concentration of genes in pathways related to mitotic nuclear division, cell division, and cell cycle (**Table 2**).

Selection and analysis of hub genes

Within the constructed PPI network of the DEGs, hub genes were identified using Cytoscape's plug-in MCODE. The six candidate hub genes, defined as genes with many interacting partners, were as follows: CDC20, Lysophosphatidic acid receptor 3 (LPAR3), CD24, LY/PLAUR domain containing 6B (LYPD6B), localized glutamic acid rich protein (MGARP), and Aldehyde oxidase1 (AOX1) (**Table 3**). The networks of hub genes and their co-expressed genes were analyzed using GeneMANIA (**Figure 2A**). Using BINGO, a biological process analysis was constructed, indicating the top5 involved BPs includes positive regulation of ubiquitin-protein ligase activity, activation of anaphase-promoting complex activity, regulation of cellular protein metabolic process, regulation of proteasomal ubiquitin-dependent protein catabolic process, regulation of molecular function (**Figure 2B**). Taken together, analysis of the six hub genes showed CDC20 to be most closely related to EOC as it was highly expressed in EOC tissue, correlated with tumor pathological type, grade, and prognosis [9, 10, 17-21].

Validation of CDC20 expression in EOC

Datasets within the Oncomine database were used to verify CDC20 expression in EOC. The difference in CDC20 expression between cancer tissues and control groups across four data sets was found to be statistically significant ($P<0.001$) (**Figure 3A**). Additionally, analysis of

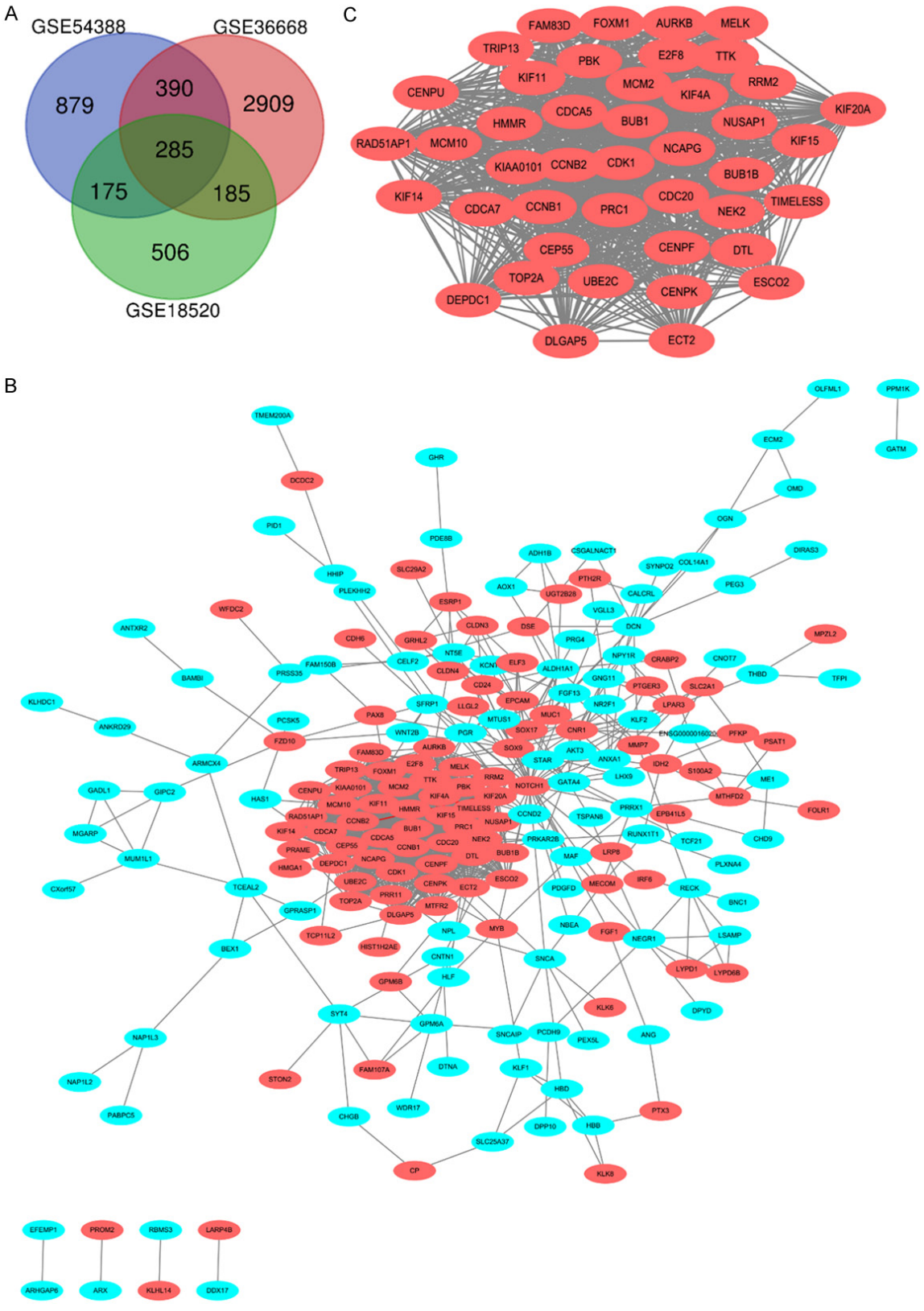

Figure 1. (A) Venn diagram of 3 datas (B) PPI network of DEGs. Up-regulated genes are marked with light red, and down-regulated genes are marked with light blue. (C) The most important module in the PPI network.

Table 1. GO and KEGG pathway enrichment analysis of DEGs in OC samples

	Term	Description	Count in gene set	*P*-value
Biological process	GO:0051301	cell division	18	8.7E-6
	GO:0007067	mitotic nuclear division	15	1.0E-5
	GO:0008283	cell proliferation	18	1.6E-5
	GO:0045944	positive regulation of transcription from RNA polymerase II promoter	29	2.5E-4
	GO:0034501	protein localization to kinetochore	4	3.0E-4
Cellular component	GO:0030496	midbody	11	1.3E-5
	GO:0005819	spindle	10	5.0E-5
	GO:0031225	anchored component of membrane	9	1.9E-4
	GO:0005876	spindle microtubule	6	3.5E-4
	GO:0009986	cell surface	17	4.0E-3
Molecular function	GO:0043565	sequence-specific DNA binding	19	3.4E-4
	GO:0008017	microtubule binding	11	6.6E-4
	GO:0019894	kinesin binding	5	1.3E-3
	GO:0019901	protein kinase binding	13	6.4E-3
	GO:0030544	HSP70 protein binding	4	1.1E-2
KEGG pathway	hsa04110	Cell cycle	9	2.3E-4
	hsa05200	Pathways in cancer	13	5.8E-3
	hsa04914	Progesterone-mediated oocyte maturation	6	6.0E-3
	hsa04310	Wnt signaling pathway	7	1.0E-2
	hsa04115	p53 signaling pathway	5	1.2E-2

Table 2. GO and KEGG pathway enrichment analysis of DEGs in the most significant module

	Term	Description	Count in gene set	*P*-value
Biological process	GO:0007067	mitotic nuclear division	15	5.8E-16
	GO:0051301	cell division	16	2.7E-15
	GO:0007062	sister chromatid cohesion	8	6.0E-9
	GO:0008283	cell proliferation	11	1.7E-8
	GO:0000086	G2/M transition of mitotic cell cycle	7	1.1E-6
Cellular component	GO:0030496	midbody	10	1.2E-11
	GO:0005654	nucleoplasm	26	6.4E-11
	GO:0005819	spindle	9	2.9E-10
	GO:0005634	nucleus	32	4.5E-9
	GO:0005876	spindle microtubule	6	5.2E-8
Molecular function	GO:0005515	protein binding	40	1.7E-9
	GO:0005524	protein binding	17	1.6E-7
	GO:0008017	microtubule binding	8	6.1E-7
	GO:0004674	protein serine/threonine kinase activity	8	3.0E-5
	GO:0003777	microtubule motor activity	5	4.1E-5
KEGG pathway	hsa04110	Cell cycle	8	1.6E-10
	hsa04114	Oocyte meiosis	5	1.9E-5
	hsa04115	p53 signaling pathway	4	1.4E-4
	hsa04914	Progesterone-mediated oocyte maturation	4	3.0E-4

CDC20 expression in cancer tissue and normal tissue within the TCGA database showed a significant statistical difference (*P*=2.44E-6) (**Figure 3B**).

Table 3. Functional roles of 6 HUB genes

Gene symbol	Full name	Function
CDC20	Cell division cycle 20	It is required for two microtubule-dependent processes, nuclear movement prior to anaphase and chromosome separation.
LPAR3	Lysophosphatidic acid receptor 3	This protein functions as a cellular receptor for lysophosphatidic acid and mediates lysophosphatidic acid-evoked calcium mobilization.
CD24	CD24 molecule	This gene encodes a sialoglycoprotein that is expressed on mature granulocytes and B cells and modulates growth and differentiation signals to these cells.
LYPD6B	LY/PLAUR domain containing 6B	Cell proliferation, migration, cell-cell interaction, immune cell maturation, macrophage activation and cytokine production.
MGARP	Mitochondria localized glutamic acid rich protein	Architecture and organization of mitochondria.
AOX1	Aldehyde oxidase1	Aldehyde oxidase produces hydrogen peroxide and, under certain conditions, can catalyze the formation of superoxide.

Furthermore, analysis of the CDC20 levels in OC tissues of different pathological types were highest in serous adenocarcinoma, as compared to levels in ovarian clear cell carcinoma, ovarian endometrioid carcinoma, and mucinous adenocarcinoma (P<0.001) (**Figure 3C**). In the Sieben ovarian database, CDC20 was significantly positively correlated with tumor grade (P<0.001) (**Figure 3D**). Additionally, disease-free survival time of the group with abnormal CDC20 was significantly shorter than that of the control group (P<0.001), as shown using the cBioPortal online platform (**Figure 3E**).

The expression of CDC20 and SOX2 in EOC cell lines

The efficacy of CDC20 shRNA knockdown was tested in human OVCAR3 ovarian cancer cells. SOX2 was used as a downstream control for CDC20 knockdown. The mRNA levels of *CDC20* and *SOX2* across all groups were similar in trend (**Figure 4A**). No significant difference was found in *CDC20* and *SOX2* mRNA levels between the control group and the shRNA NC control group. Yet, CDC20 expression was significantly decreased within the CDC20 shRNA01, shRNA02, and shRNA03 groups as compared to controls (P<0.05). Protein levels of CDC20 and SOX2 in the CDC20 shRNA02 group were significantly lower than those in the other groups (P<0.05) (**Figure 4B**).

The effect of silencing CDC20 on proliferation of EOC cells

The CCK8 assay was used to determine the effect of CDC20 knockdown on cell proliferation. Cell proliferation in the CDC20 shRNA02 group was significantly lower than that in the other groups (P<0.05). There was no statistical difference between the CDC20 shRNA01 and shRNA03 groups compared with the control and shRNA NC groups (P≥0.05) (**Figure 4C**). Additionally, decreased mRNA levels of the *Cyclin D1* and *Cyclin D2* genes, which regulate tumor cell proliferation, were observed after CDC20 knockdown (**Figure 4F**).

The effect of silencing CDC20 on apoptosis of EOC cells

The CDC20 shRNA02 group showed a significantly higher number of apoptotic cells than other groups (P<0.05). There was no statistical difference between the CDC20 shRNA01 group and the CDC20 shRNA03 group compared with control and shRNA NC groups (P≥0.05) (**Figure 4D**). Furthermore, mRNA levels of the pro-apoptotic gene *BAX* were increased and mRNA levels of the anti-apoptotic gene *BCL-2* were decreased after CDC20 knockdown (**Figure 4F**).

The effect of silencing CDC20 on metastasis of EOC cells

Transwell experiments tested the effects of CDC20 on cell motility. After CDC20 knockdown, the number of EOC cells penetrating the membrane was significantly less than those in the shRNA NC group (**Figure 4E**). In all transfected groups, mRNA levels of *E-cadherin*, an epithelial-mesenchymal transition-related gene, increased (**Figure 4F**).

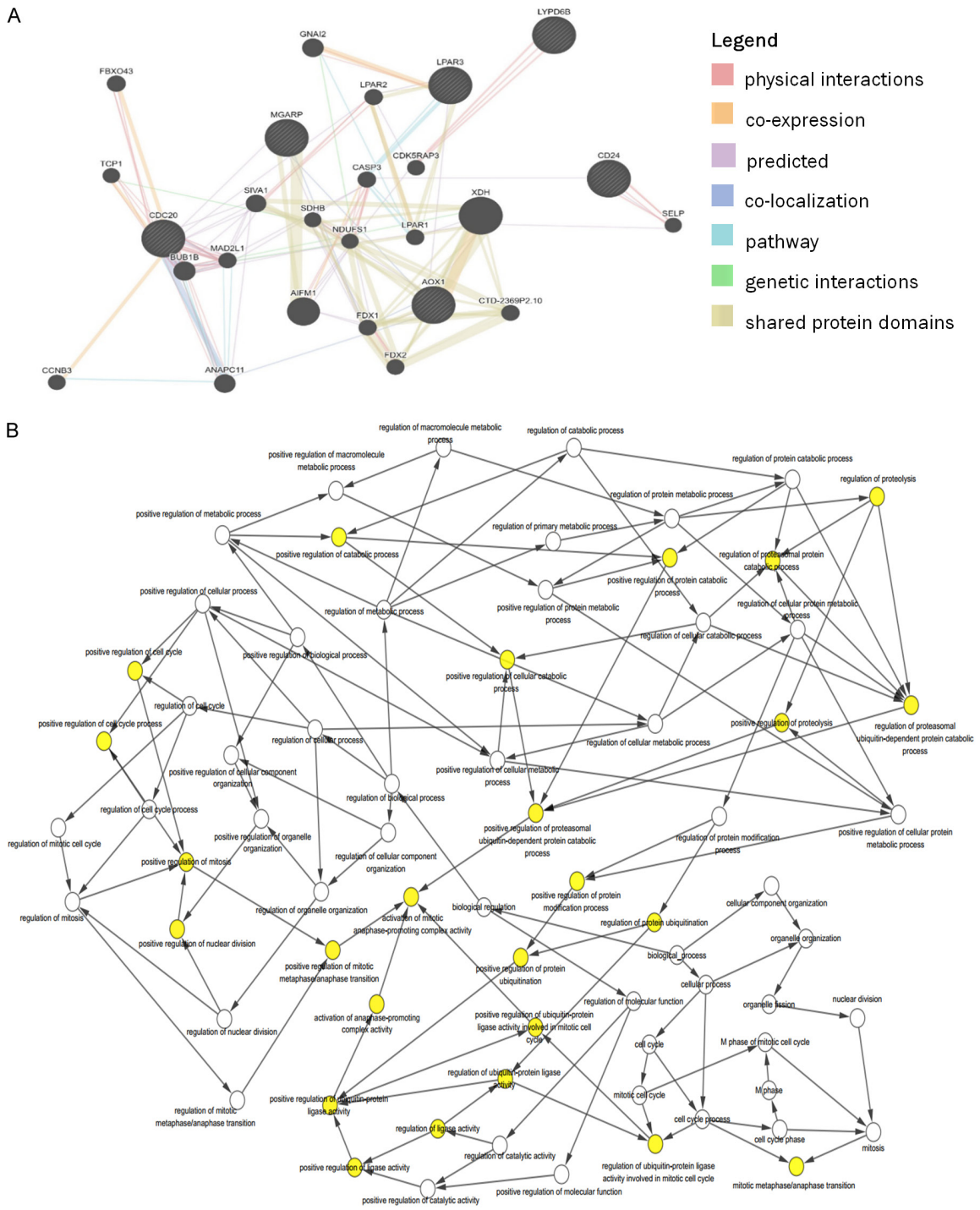

Figure 2. A. Hub genes and their co-expression genes were analyzed using GENEMANIA. B. The biological process analysis of hub genes was constructed using BINGO. The color depth of each node refers to the corrected *P* value of the ontology. The size of each node refers to the number of genes involved in the ontology. $P<0.01$ was considered statistically significant.

Discussion

Tumors are heterogeneous diseases characterized by multiple genetic abnormalities. Despite years of research, the pathogenesis of EOC remains unclear. Recent decades have seen high-throughput techniques widely applied to cancer research, such as those to measure

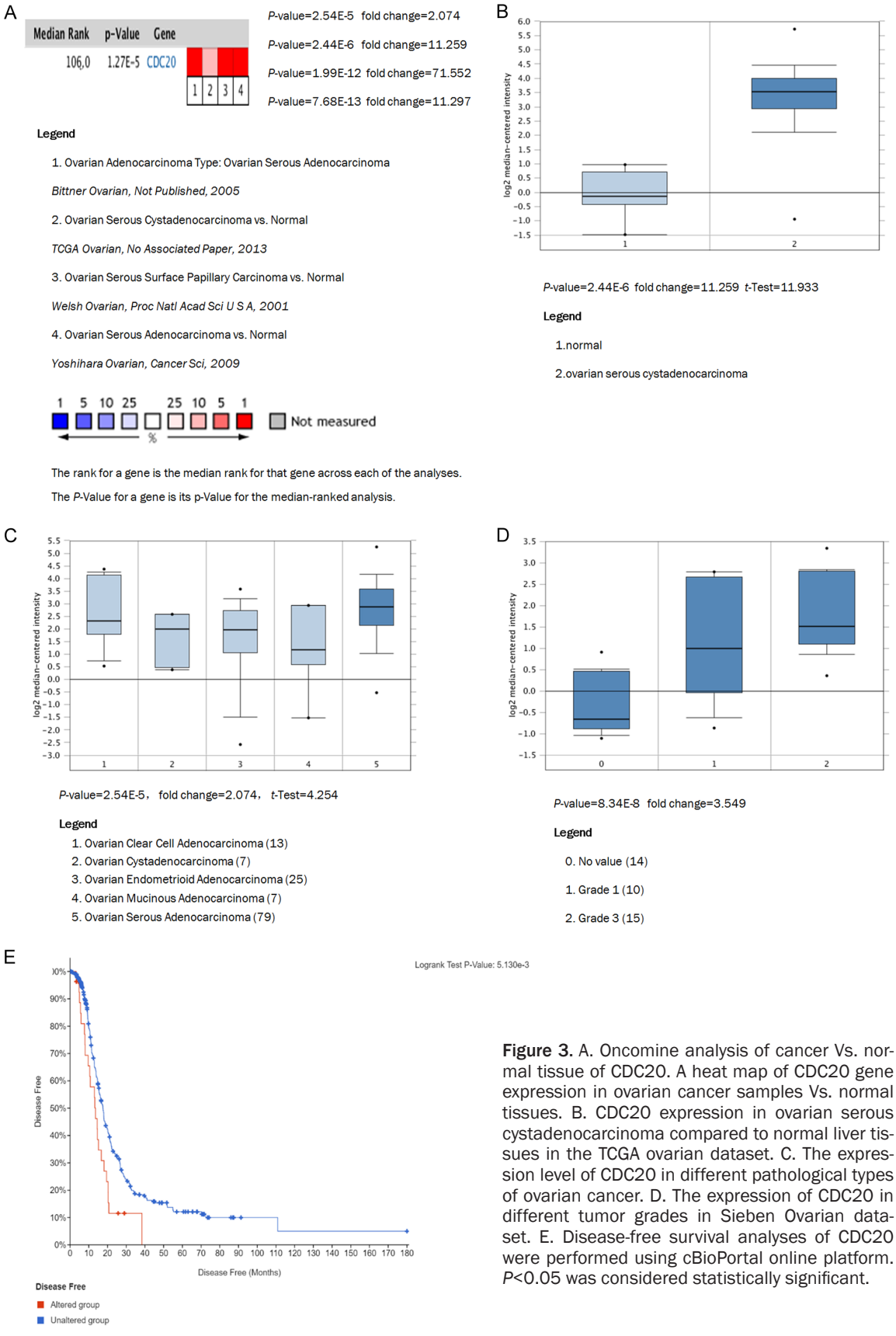

Figure 3. A. Oncomine analysis of cancer Vs. normal tissue of CDC20. A heat map of CDC20 gene expression in ovarian cancer samples Vs. normal tissues. B. CDC20 expression in ovarian serous cystadenocarcinoma compared to normal liver tissues in the TCGA ovarian dataset. C. The expression level of CDC20 in different pathological types of ovarian cancer. D. The expression of CDC20 in different tumor grades in Sieben Ovarian dataset. E. Disease-free survival analyses of CDC20 were performed using cBioPortal online platform. $P<0.05$ was considered statistically significant.

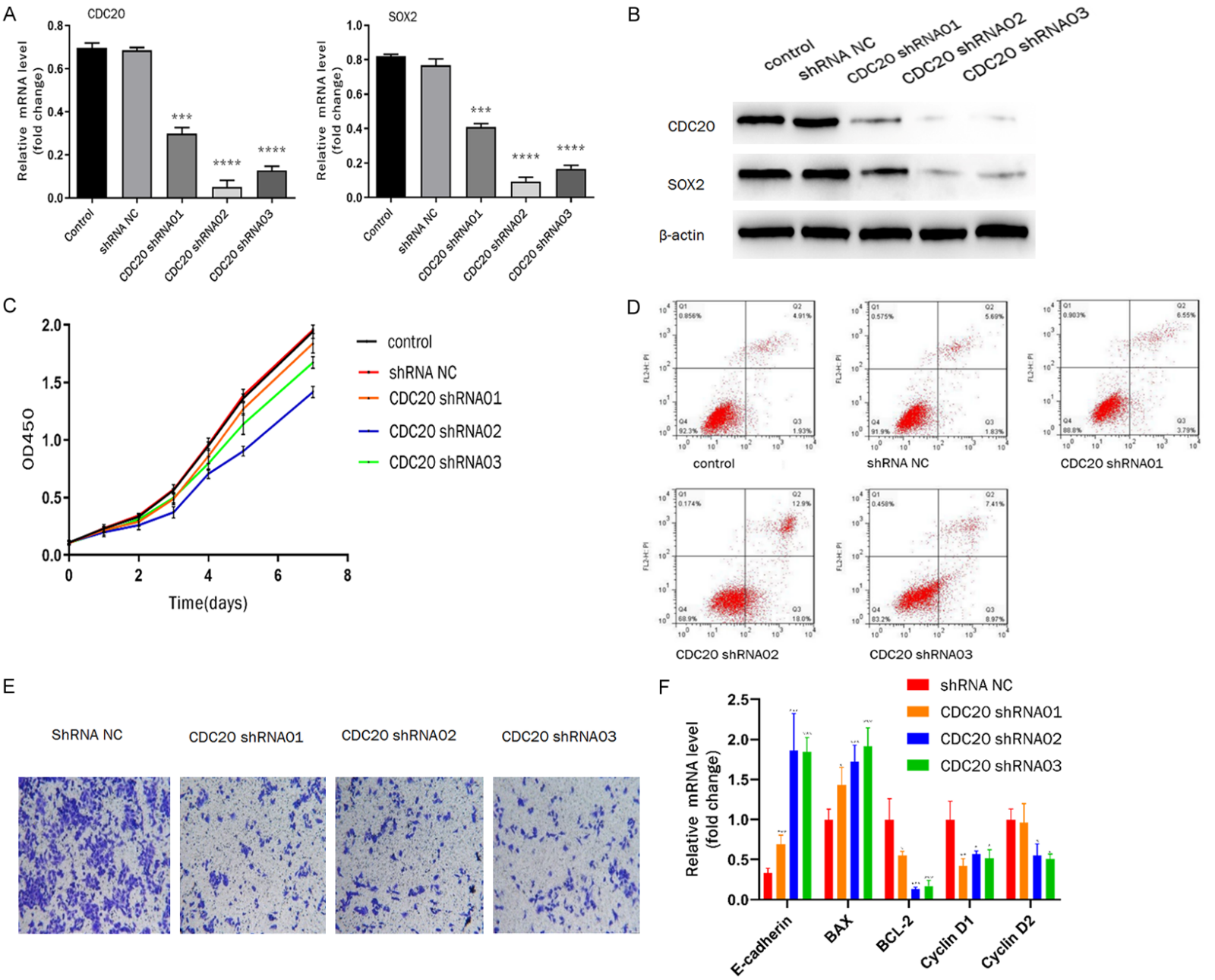
A
CDC20
SOX2
Relative mRNA level (fold change)
Control
shRNA NC
CDC20 shRNA01
CDC20 shRNA02
CDC20 shRNA03
B
control
shRNA NC
CDC20 shRNA01
CDC20 shRNA02
CDC20 shRNA03
CDC20
SOX2
β-actin
C
OD450
Time(days)
control
shRNA NC
CDC20 shRNA01
CDC20 shRNA02
CDC20 shRNA03
D
control
shRNA NC
CDC20 shRNA01
CDC20 shRNA02
CDC20 shRNA03
E
ShRNA NC
CDC20 shRNA01
CDC20 shRNA02
CDC20 shRNA03
F
shRNA NC
CDC20 shRNA01
CDC20 shRNA02
CDC20 shRNA03
Relative mRNA level (fold change)
E-cadherin
BAX
BCL-2
Cyclin D1
Cyclin D2

Figure 4. A. qRT-PCR detection of CDC20 and SOX2 expression in ovarian cancer cell lines. B. Western blot detection of CDC20 and SOX2 expression in ovarian cancer cell lines. C. Proliferation ability of ovarian cancer cells after silencing CDC20. D. Quadrant of apoptosis in flow cytometry. E. Transwell assays to investigate migratory ablilities of ovarian cancer cell lines transfected with shRNA-NC or shRNA01, 02, 03. Sample size =4. F. qRT-PCR detection of E-cadherin, BAX, BCL-2, Cyclin D1 and Cyclin D2 expression in ovarian cancer cell lines. $^{****}P<0.0001$, $^{***}P<0.001$, $^{*}P<0.05$, compared with shRNA-NC.

RNA intermediates and epigenetic marks, including protein modifications and DNA methylation [22]. The rapid development of gene chip and bioinformatic analysis technologies have allowed extensive mining of genome level expression changes to identify genes and pathways related to tumorigenesis and prognosis [23].

This study found over 6,000 genes differentially expressed between EOC tissue and normal ovarian tissue, with 259 genes shared across three independent samples. Importantly, bioinformatic analysis uncovered six hub genes: CDC20, LPAR3, CD24, LYPD6B, MGARP, and AOX1, which show high interconnectedness to other genes within the PPI network. Of these hub genes, CDC20 shows high expression in EOC tissue, and correlates with tumor pathological type, grade, and prognosis [10, 19-21, 24]. CDC20 is a prospective key biomarker for EOC with possible uses in early clinical detection, prognostic evaluation, and therapeutic targeting [25].

The regulatory role of CDC20 in the cell cycle

As a regulator of anaphase-promoting complex or cyclosome (APC/C), CDC20 plays a key regulatory role in chromosome segregation and mitotic exit [11]. The many roles APC/C plays in the cell make it of great interest to research oncologists. Initially thought only to regulate the cell cycle, the multifunctional ubiquitin protein ligase APC/C ubiquitinates various substrates to regulate cell division, differentiation, genome stabilization, energy metabolism, cell death, autophagy and carcinogenesis, and other cellular processes [26, 27]. The APC/C function of cell cycle regulation is mainly controlled by two co-activators: CDC20 and E-cadherin (CDH1). Although APC/C^{CDC20} and APC/C^{CDH1} have some substrate overlap, APC/C^{CDC20} mainly controls metaphase-to-anaphase shift and mitotic exit, whereas APC/C^{CDH1} is active primarily in anaphase of mitotic exit and early G1 [28].

CDC20 plays another important role in cell cycle control as a target of the spindle assembly checkpoint (SAC). The SAC is a complex signaling system that monitors the mitotic process to ensure all chromosomes properly attach to spindle microtubules. The SAC response involves interaction with the kinetochore, which is a multi-protein structure that connects chromosomes to microtubule polymers to pull sister chromatids apart during cell division. Defects in this chromosome segregation process can lead to aneuploidy, a common feature of cancer cells [29]. Recruitment of the SAC protein to the centromere induces a conformational change in mitotic arrest deficient-like 2 (MAD2) to the closed conformation (C-MAD2). C-MAD2 promotes the production of the mitotic checkpoint complex (MCC), which is composed of CDC20, BubR1 and Bub3. MCC promotes the inactivation of APC/C^{CDC20} [9, 30]. Once all kinetochores properly attach to microtubules, the degradation of MCC permits APC/C^{CDC20} to allow mitosis to continue and achieve the G2/M phase transition [31].

CDC20 regulation of apoptosis

In addition to regulating mitotic progression, CDC20 also participates in apoptosis. CDC20 targets both Myeloid cell leukemia-1 (MCL-1) and Bcl-2 interacting mediator of cell death (BIM) [32]. Members of the B-cell lymphoma-2 (BCL-2) protein family influence apoptosis pathways both positively and negatively. Anti-apoptotic members include BCL-2, BCL-xl, BCL-w, and MCL-1, while Bax, Bak, and BH3-Only proteins, such as BIM, play pro-apoptotic roles [33]. Notably, BIM has attracted attention as a key regulator of apoptosis. E3 ligases have been reported to negatively regulate the stability of BIM [34]. Interestingly, research has shown APC^{CDC20}, an E3 ligase, controls the ubiquitination and destruction of BIM. During mitosis, when APC^{CDC20} is most active, the abundance of BIM decreased significantly. Additionally, depletion of CDC20 in different cell lines significantly upregulated BIM abundance

[35]. Also, CDC20 has been shown to interact with BIM through its C-terminal WD40 domain [36].

The role of CDC20 in human malignancies

In addition to the cell cycle and apoptosis, CDC20 also influences cancer initiation and progression. CDC20 plays a role in pancreatic cancer [37], breast cancer [38], prostate cancer [39], lung cancer [14], colorectal cancer [40], liver cancer [41, 42], glioma [43], gastric cancer [44], bladder cancer [45], cervical cancer [46] and other human tumors [12, 24]. Overexpression of CDC20 can be associated with poor prognosis in tumor patients [47]. Meta-analysis of eight studies (n=1856 cases) revealed a relationship between CDC20 overexpression and overall survival (OS) in human solid tumors. Univariate and multivariate survival analysis showed that patients with high CDC20 expression had significantly shorter OS. In univariate analysis, the hazard ratio (HR) for OS was 1.75 (95% CI: 1.07-2.86, P=0.03). The HR of OS multivariate analysis was 2.48 (95% CI: 2.10-2.94, P<0.001) [24]. Thus, in addition to being an important marker to determine prognosis, CDC20 may also serve as a therapeutic target for solid tumors.

CDC20 overexpression allows tumor cells to bypass SAC surveillance and exit the mitotic process prematurely, resulting in genomic instability [13]. CDC20 overexpression also associates with Wnt/β-catenin pathway activation, a pathway closely related to cancer progression [12, 48]. Activated Wnt protein induces the nuclear translocation of β-catenin, which interacts with the T-cell factors/lymphoid enhancing factor (TCF/LEF) family to activate genes including stromelysin, fibroblast growth factor, epidermal growth factor, cyclin D, and CD44 [49]. Inhibition of CDC20 expression in skin cancer by interfering RNA results in decreased β-catenin [12]. Although a direct interaction between CDC20 and β-catenin was not shown, it is clear that CDC20 influences β-catenin regulation.

In addition, CDC20 may play an important role in tumor recurrence and metastasis through cancer stem-like cells (CSCs)/tumor initiating cells (TICs) [50]. The tumor-promoting mechanism of CDC20 in CSCS/TICs may be achieved through the SOX2 signaling pathway [51]. As an important transcription factor, SOX2 is associated with the stemness of pluripotent stem cells and also plays a key role in regulating the self-renewal and stemness in CSCs [52]. In glioblastoma, APC/C^{CDC20} forms a complex with SOX2 and maintains its stability, which contributes to the self-renewal of tumor cells [16].

The relationship between CDC20 and SOX2

This study explored a potential role of CDC20 as an upstream regulator of SOX2 in EOC. Yet, additional experiments are needed to confirm the effects of CDC20 on the proliferation and apoptosis of EOC cells through SOX2 signaling. Future experiments to explore CDC20 overexpression effects on SOX2 levels, as well as the effects of overexpression or knockdown of CDC20 in EOC cell lines would further elucidate the relationship between CDC20 and SOX2 in cancer progression.

The mechanism by which CDC20 could regulate SOX2 remains unknown. t APC/C^{CDC20} could have an indirect influence on SOX2 through ubiquitination-mediated disruption of the key E3 ligase targeting SOX2 [16]. Another possibility is that APC/C^{CDC20} alters SOX2 stability through alterations to post-translational modifications on SOX2 [53]. Interestingly, the APC/C^{CDC20} inhibitor, proTAME reduces SOX2 levels, which suggests involvement of APC/C^{CDC20} in SOX2 regulation [27]. Understanding how APC/C^{CDC20} mediates SOX2 in EOC progression requires further cellular and animal experiments.

Study limitations

The bioinformatic nature of this study, although informative, creates some limitations. Only one tumor type, EOC, was analyzed in this study because of the availability of complete datasets and large numbers of specimens. Although EOC accounts for the majority (60-90%) of tumor types, there are other histological types of ovarian tumors. To address this limitation, CDC20 expression was analyzed in other OC histopathological types using the TCGA database. Higher CDC20 expression was found in serous OC than that in other types. Another limitation, due to lack of access to patients, is that this study has not validated CDC20 expression levels in patients with OC. More clinical and experimental work is needed to assess CDC20 levels in serum, cancer tissues, and

adjacent tissues in patients with different types of OC. Only after large-scale, multi-center clinical research CDC20 will be ready for use in early screening and prognostic evaluation.

Conclusions

In summary, bioinformatics analysis of three public databases revealed significant upregulation of CDC20 levels in EOC tissues. These CDC20 levels correlated with tumor pathological type, grade, and prognosis. Furthermore, the effects of CDC20 on OC cell proliferation, apoptosis, metastasis and possible signaling pathways were explored in an OC cell line. Taken together, these findings can help build a knowledge base for clinicians to facilitate early diagnosis, individualize treatment options, and improve prognosis for OC patients.

Acknowledgements

This work was funded by Scientific Research Project of Gusu School of Nanjing Medical University (No. GSKY20210208), "Science and Education Revitalize Health" Youth Science and Technology Project of Suzhou (NO. KJXW2020028), Municipal hospital gynecological clinical trial and improvement Project of Suzhou (No. SLT201955).

Disclosure of conflict of interest

None.

Address correspondence to: Shunyu Hou, Department of Obstetrics and Gynaecology, The Affiliated Suzhou Hospital of Nanjing Medical University, Suzhou Municipal Hospital, Gusu School, Nanjing Medical University, Suzhou 215002, Jiangsu, China. Tel: +86-13962179232; +86-512-6236-2003; E-mail: houshunyu@sina.com

References

[1] Park JY, Lee JY, Lee YY, Shim SH, Suh DH and Kim JW. Major clinical research advances in gynecologic cancer in 2021. J Gynecol Oncol 2022; 33: e43.

[2] Atallah GA, Abd Aziz NH, Teik CK, Shafiee MN and Kampan NC. New predictive biomarkers for ovarian cancer. Diagnostics (Basel) 2021; 11: 465.

[3] Bonifacio VDB. Ovarian cancer biomarkers: moving forward in early detection. Adv Exp Med Biol 2020; 1219: 355-363.

[4] Harbin LM, Gallion HH, Allison DB and Kolesar JM. Next generation sequencing and molecular biomarkers in ovarian cancer-an opportunity for targeted therapy. Diagnostics (Basel) 2022; 12: 842.

[5] Chandra A, Pius C, Nabeel M, Nair M, Vishwanatha JK, Ahmad S and Basha R. Ovarian cancer: current status and strategies for improving therapeutic outcomes. Cancer Med 2019; 8: 7018-7031.

[6] Tsang SI, Hassan AA, To SKY and Wong AST. Experimental models for ovarian cancer research. Exp Cell Res 2022; 416: 113150.

[7] Dong CC, Tian X, He FC, Zhang JY, Cui XJ, He Q, Si P and Shen YM. Integrative analysis of key candidate genes and signaling pathways in ovarian cancer by bioinformatics. J Ovarian Res 2021; 14: 92.

[8] Yoon H and Lee S. Integration of genomic profiling and organoid development in precision oncology. Int J Mol Sci 2021; 23: 216.

[9] Belur Nagaraj A, Kovalenko O, Avelar R, Joseph P, Brown A, Surti A, Mantilla S and DiFeo A. Mitotic exit dysfunction through the deregulation of APC/C characterizes cisplatin-resistant state in epithelial ovarian cancer. Clin Cancer Res 2018; 24: 4588-4601.

[10] Fei HJ, Chen SC and Xu CM. Bioinformatics analysis of gene expression profile of serous ovarian carcinomas to screen key genes and pathways. J Ovarian Res 2020; 13: 82.

[11] McLean JR, Chaix D, Ohi MD and Gould KL. State of the APC/C: organization, function, and structure. Crit Rev Biochem Mol Biol 2011; 46: 118-136.

[12] Chu ZW, Zhang XY, Li QY, Hu GL, Lian CG and Geng SM. CDC20 contributes to the development of human cutaneous squamous cell carcinoma through the Wnt/betacatenin signaling pathway. Int J Oncol 2019; 54: 1534-1544.

[13] Kapanidou M, Curtis NL and Bolanos-Garcia VM. Cdc20: at the crossroads between chromosome segregation and mitotic exit. Trends Biochem Sci 2017; 42: 193-205.

[14] Kato T, Daigo Y, Aragaki M, Ishikawa K, Sato M and Kaji M. Overexpression of CDC20 predicts poor prognosis in primary non-small cell lung cancer patients. J Surg Oncol 2012; 106: 423-430.

[15] Akter S, Rahman MA, Hasan MN, Akhter H, Noor P, Islam R, Shin Y, Rahman MDH, Gazi MS, Huda MN, Nam NM, Chung J, Han S, Kim B, Kang I, Ha J, Choe W, Choi TG and Kim SS. Recent advances in ovarian cancer: therapeutic strategies, potential biomarkers, and technological improvements. Cells 2022; 11: 650.

[16] Mao DD, Gujar AD, Mahlokozera T, Chen I, Pan Y, Luo J, Brost T, Thompson EA, Turski A, Leuthardt EC, Dunn GP, Chicoine MR, Rich KM,

Dowling JL, Zipfel GJ, Dacey RG, Achilefu S, Tran DD, Yano H and Kim AH. A CDC20-APC/SOX2 signaling axis regulates human glioblastoma stem-like cells. Cell Rep 2015; 11: 1809-1821.

[17] Del Valle I, Buonocore F, Duncan AJ, Lin L, Barenco M, Parnaik R, Shah S, Hubank M, Gerrelli D and Achermann JC. A genomic atlas of human adrenal and gonad development. Wellcome Open Res 2017; 2: 25.

[18] Koroknai V, Szasz I, Hernandez-Vargas H, Fernandez-Jimenez N, Cuenin C, Herceg Z, Vizkeleti L, Adany R, Ecsedi S and Balazs M. DNA hypermethylation is associated with invasive phenotype of malignant melanoma. Exp Dermatol 2020; 29: 39-50.

[19] Onallah H, Davidson B and Reich R. Diverse effects of lysophosphatidic acid receptors on ovarian cancer signaling pathways. J Oncol 2019; 2019: 7547469.

[20] Zhao L, Li YH, Zhang Z, Zou J, Li JF, Wei R, Guo Q, Zhu XX, Chu C, Fu XX, Yue JB and Li X. Meta-analysis based gene expression profiling reveals functional genes in ovarian cancer. Biosci Rep 2020; 40: BSR20202911.

[21] Zou J, Li YK, Liao NC, Liu J, Zhang QF, Luo M, Xiao J, Chen YH, Wang MJ, Chen KX, Zeng J and Mo ZC. Identification of key genes associated with polycystic ovary syndrome (PCOS) and ovarian cancer using an integrated bioinformatics analysis. J Ovarian Res 2022; 15: 30.

[22] Zhao YZ, Pi J, Liu LH, Yan WJ, Ma SF and Hong L. Identification of the hub genes associated with the prognosis of ovarian cancer patients via integrated bioinformatics analysis and experimental validation. Cancer Manag Res 2021; 13: 707-721.

[23] Kumar SU, Kumar DT, Siva R, Doss CGP and Zayed H. Integrative bioinformatics approaches to map potential novel genes and pathways involved in ovarian cancer. Front Bioeng Biotechnol 2019; 7: 391.

[24] Wang SJ, Chen BR, Zhu ZP, Zhang L, Zeng JJ, Xu GX, Liu G, Xiong DS, Luo Q and Huang ZJ. CDC20 overexpression leads to poor prognosis in solid tumors: a system review and meta-analysis. Medicine (Baltimore) 2018; 97: e13832.

[25] Yang W, Kim D, Kim DK, Choi KU, Suh DS and Kim JH. Therapeutic Strategies for targeting ovarian cancer stem cells. Int J Mol Sci 2021; 22: 5059.

[26] Alfieri C, Zhang SY and Barford D. Visualizing the complex functions and mechanisms of the anaphase promoting complex/cyclosome (APC/C). Open Biol 2017; 7: 170204.

[27] Schrock MS, Stromberg BR, Scarberry L and Summers MK. APC/C ubiquitin ligase: functions and mechanisms in tumorigenesis. Semin Cancer Biol 2020; 67: 80-91.

[28] Alfieri C, Chang LF, Zhang ZG, Yang J, Maslen S, Skehel M and Barford D. Molecular basis of APC/C regulation by the spindle assembly checkpoint. Nature 2016; 536: 431-436.

[29] Sansregret L, Patterson JO, Dewhurst S, Lopez-Garcia C, Koch A, McGranahan N, Chao WCH, Barry DJ, Rowan A, Instrell R, Horswell S, Way M, Howell M, Singleton MR, Medema RH, Nurse P, Petronczki M and Swanton C. APC/C dysfunction limits excessive cancer chromosomal instability. Cancer Discov 2017; 7: 218-233.

[30] Das T, Roy KS, Chakrabarti T, Mukhopadhyay S and Roychoudhury S. Withaferin A modulates the Spindle assembly checkpoint by degradation of Mad2-Cdc20 complex in colorectal cancer cell lines. Biochem Pharmacol 2014; 91: 31-39.

[31] Barford D. Structural interconversions of the anaphase-promoting complex/cyclosome (APC/C) regulate cell cycle transitions. Curr Opin Struct Biol 2020; 61: 86-97.

[32] Allan LA, Skowyra A, Rogers KI, Zeller D and Clarke PR. Atypical APC/C-dependent degradation of Mcl-1 provides an apoptotic timer during mitotic arrest. EMBO J 2018; 37: e96831.

[33] Cosialls AM, Sanchez-Vera I, Pomares H, Perramon-Andujar J, Sanchez-Esteban S, Palmeri CM, Iglesias-Serret D, Saura-Esteller J, Nunez-Vazquez S, Lavilla R, Gonzalez-Barca EM, Pons G and Gil J. The BCL-2 family members NOXA and BIM mediate fluorizoline-induced apoptosis in multiple myeloma cells. Biochem Pharmacol 2020; 180: 114198.

[34] Wan LX, Tan MJ, Yang J, Inuzuka H, Dai XP, Wu T, Liu J, Shaik S, Chen GA, Deng J, Malumbres M, Letai A, Kirschner MW, Sun Y and Wei WY. APC(Cdc20) suppresses apoptosis through targeting Bim for ubiquitination and destruction. Dev Cell 2014; 29: 377-391.

[35] Shang GN, Ma X and Lv G. Cell division cycle 20 promotes cell proliferation and invasion and inhibits apoptosis in osteosarcoma cells. Cell Cycle 2018; 17: 43-52.

[36] Wu F, Lin Y, Cui P, Li HY, Zhang LC, Sun ZQ, Huang SL, Li S, Huang SM, Zhao QL and Liu QY. Cdc20/p55 mediates the resistance to docetaxel in castration-resistant prostate cancer in a Bim-dependent manner. Cancer Chemother Pharmacol 2018; 81: 999-1006.

[37] Zhang Y, Xue YB, Li H, Qiu D, Wang ZW and Tan SS. Inhibition of cell survival by curcumin is associated with downregulation of cell division cycle 20 (Cdc20) in pancreatic cancer cells. Nutrients 2017; 9: 109.

[38] Parmar MB, K C RB, Lobenberg R and Uludag H. Additive polyplexes to undertake siRNA therapy against CDC20 and survivin in breast cancer cells. Biomacromolecules 2018; 19: 4193-4206.

[39] Li K, Mao YH, Lu L, Hu C, Wang DJ, Si-Tu J, Lu MH, Peng SB, Qiu JG and Gao X. Silencing of CDC20 suppresses metastatic castration-resistant prostate cancer growth and enhances chemosensitivity to docetaxel. Int J Oncol 2016; 49: 1679-1685.

[40] Li JX, Wang YC, Wang X and Yang QQ. CDK1 and CDC20 overexpression in patients with colorectal cancer are associated with poor prognosis: evidence from integrated bioinformatics analysis. World J Surg Oncol 2020; 18: 50.

[41] Yang G, Wang G, Xiong YF, Sun J, Li WN, Tang T and Li JD. CDC20 promotes the progression of hepatocellular carcinoma by regulating epithelialmesenchymal transition. Mol Med Rep 2021; 24: 483.

[42] Zheng YC, Shi Y, Yu S, Han YY, Kang K, Xu HF, Gu HJ, Sang XT, Chen Y and Wang JY. GTSE1, CDC20, PCNA, and MCM6 synergistically affect regulations in cell cycle and indicate poor prognosis in liver cancer. Anal Cell Pathol (Amst) 2019; 2019: 1038069.

[43] Zhang YQ, Li JY, Yi KK, Feng J, Cong ZM, Wang Z, Wei YF, Wu F, Cheng W, Samo AA, Salomoni P, Yang Q, Huang Y, Kang CS, Jiang T and Fan XL. Elevated signature of a gene module coexpressed with CDC20 marks genomic instability in glioma. Proc Natl Acad Sci U S A 2019; 116: 6975-6984.

[44] Wang LX, Zhang JF, Wan LX, Zhou XX, Wang ZW and Wei WY. Targeting Cdc20 as a novel cancer therapeutic strategy. Pharmacol Ther 2015; 151: 141-151.

[45] Wang LX, Yang CL, Chu M, Wang ZW and Xue BX. Cdc20 induces the radioresistance of bladder cancer cells by targeting FoxO1 degradation. Cancer Lett 2021; 500: 172-181.

[46] Chen ZH, Jing YJ, Yu JB, Jin ZS, Li Z, He TT and Su XZ. ESRP1 induces cervical cancer cell G1-Phase arrest via regulating cyclin A2 mRNA stability. Int J Mol Sci 2019; 20: 3705.

[47] Choi JW, Kim Y, Lee JH and Kim YS. High expression of spindle assembly checkpoint proteins CDC20 and MAD2 is associated with poor prognosis in urothelial bladder cancer. Virchows Arch 2013; 463: 681-687.

[48] Li J, Karki A, Hodges KB, Ahmad N, Zoubeidi A, Strebhardt K, Ratliff TL, Konieczny SF and Liu XQ. Cotargeting polo-like Kinase 1 and the Wnt/beta-catenin signaling pathway in castration-resistant prostate cancer. Mol Cell Biol 2015; 35: 4185-4198.

[49] Zhang Q, Huang H, Liu A, Li J, Liu CY, Sun B, Chen L, Gao Y, Xu DF and Su CQ. Cell division cycle 20 (CDC20) drives prostate cancer progression via stabilization of beta-catenin in cancer stem-like cells. EBioMedicine 2019; 42: 397-407.

[50] Zeng H, Ji JR, Song XD, Huang YQ, Li H, Huang J and Ma XL. Stemness related genes revealed by network analysis associated with tumor immune microenvironment and the clinical outcome in lung adenocarcinoma. Front Genet 2020; 11: 549213.

[51] Zheng WB, Yang CZ, Qiu L, Feng XC, Sun K and Deng HJ. Transcriptional information underlying the generation of CSCs and the construction of a nine-mRNA signature to improve prognosis prediction in colorectal cancer. Cancer Biol Ther 2020; 21: 688-697.

[52] Novak D, Huser L, Elton JJ, Umansky V, Altevogt P and Utikal J. SOX2 in development and cancer biology. Semin Cancer Biol 2020; 67: 74-82.

[53] Gujar AD, Yano H and Kim AH. The CDC20-APC/SOX2 signaling axis: an achilles' heel for glioblastoma. Mol Cell Oncol 2015; 3: e1075644.